ELEVENTH EUROPEAN ROTORCRAFT FORUM

Paper No. 25

UNSTEADY SWEEP
A KEY TO SIMULATION OF
THREE-DIMENSIONAL ROTOR BLADE AIRLOADS

Ulrich Leiss

Universität der Bundeswehr München

September 10-13, 1985
London, England.

THE CITY UNIVERSITY, LONDON, EC1V OHB, ENGLAND.

UNSTEADY SWEEP - A KEY TO SIMULATION OF THREEDIMENSIONAL ROTOR BLADE AIRLOADS

Ulrich Leiss

Universität der Bundeswehr
Institut für Luftfahrttechnik
München, Germany

Abstract

A twodimensional semi-empirical model exists for simulation of aerodynamic coefficients at arbitrary angles of attack and Mach numbers. The developed structure was modular to include threedimensional effects. First of all the steady influence of the radial flow component is considered in a manner consistent with the fundamental twodimensional formulation. Next tip losses are accounted for by a continuous reduction function due to the aspect ratio. Finally parameters are introduced as low order functions of the radial blade coordinate. Consequently fixed blade elements are no longer necessary. Analytical radial integration of aerodynamic coefficients is presented.
The unsteady sweep is derived on this steady physical basis. Recent experiments on swept oscillating airfoils are used to simulate the dominating viscous effects. Dynamic sweep plays an important role interacting with the twodimensional unsteady phenomenas. It is shown how the developed formulation can be a general aerodynamic module for the next generation real time simulation analyses.

Notation

A	total blade area
b	wing half span
c	blade chord
c_i	aerodynamic or other coefficients
F_i	total blade forces
k	reduced frequency
M_i	total blade moments
M	Mach number
q_a	dynamic sonic pressure
Re	Reynolds number
x,y,z	rotor blade fixed coordinates

Definitions:

$\dot{}$	d/dt
$\ddot{}$	d^2/dt^2
f( )	function of

α	angle of attack
$\bar{\alpha}$	amplitude of oscillation
μ	advance ratio
ω	rotor rotational frequency
ψ	azimuth angle
Λ	aspect ratio
Γ	circulation
ϕ	sweep angle

Subscripts:

c	chord
i	numbering index
l	lift
n	normal force
ss	static stall
x,y,z	coordinate direction

1. Introduction

For the flight mechanic simulation and predesign of helicopters a modular and consistent aerodynamic analysis is required. On the one hand strong limitations exist in computation time and on the other hand a lot of complex effects should be included for acceptable simulation fidelity. Modern rotors are heavily loaded and almost everything on the rotor is unsteady. The list of publications is long concerning special phenomenas but simplifications made in one case are sometimes main parameters in another one.
Therefore Johnson(1) developed a comprehensive rotorcraft analysis for a wide variety of applications and gave the direction for further development.
A significant progress has been achieved in the field of real time helicopter simulation. State of the art is now a blade element rotor model with blade degrees of freedom but the classical aerodynamic formulation still remains.(2),(3)
For the present purpose a new twodimensional model (4),(5) was presented to describe the aerodynamic forces and moments of a rotor blade. Special emphasis was given to unsteady effects.
In the present investigation the model was extended to include the steady and unsteady threedimensional influence. The objectives were to use simple theory if available and empirical parameters with physical background. Analytical expressions were necessary to obtain exact integration in radial blade direction.
First of all the third component of the freestream velocity was investigated. Critical review of steady and unsteady swept wing experiments results in the nonvalidity of the well known independence principle for the helicopter case. This fact leads to a steady sweep model which accounts for the viscous effects of yawed flow. One is the delay of stall to higher angles of attack the other a decrease of lift curve slope. This behaviour is referred to the plane normal to the leading edge. Till now experiments were performed with constant sweep and oscillating angle of attack but not reverse. Yawed flow is never steady on a helicopter rotor and therefore the unsteady viscous sweep effect alters the simultaneous ongoing dynamic stall behaviour. A preliminary model was presented to simulate this effect.

Next the finite length of a rotor blade is considered. The circulation is reduced to zero at the tip and the root of the blade. A sheet of trailed vorticity reduces the angle of attack and consequently the circulation. A continuous reduction function gives appropriate results for different load distributions and aspect ratios.
Parameters of the whole aerodynamic model are formulated as low order functions of the radial coordinate. Analytical integration is obtained and supported by the modular structure and the superposition principle.

2. Definition Of The Problem

The coordinate system of the present method is cartesian in contrast to the classical formulation of sectional aerodynamics. This convenient assumption is shown in Fig.1.

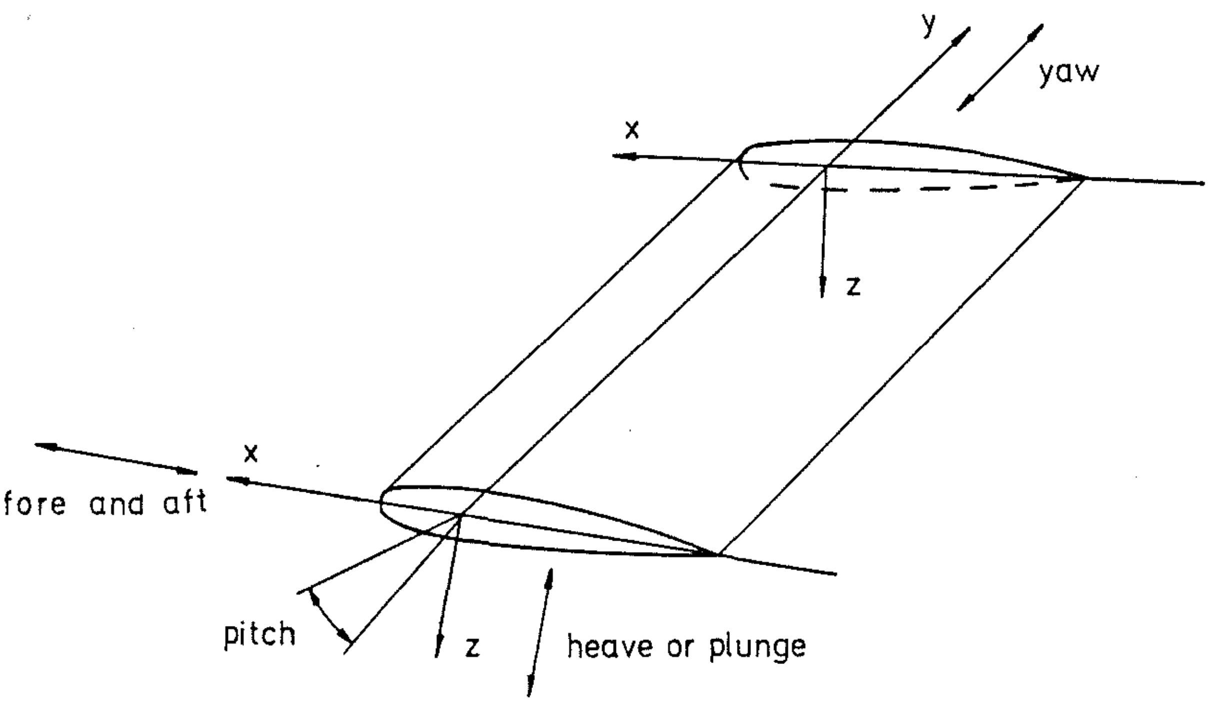

Fig.1 Rotor blade coordinates and types of motion

The general purpose of the method is to obtain the total aerodynamic forces and moments in the origin of the coordinate system.

$$F_i,\ M_i \ = \ c_i \cdot q_a \cdot A_{bl}$$

The generalized nondimensional aerodynamic coefficients c_i depend in the steady case only on the velocities.

$$c_{i\ \text{steady}} = f(\dot{x},\dot{y},\dot{z})$$

The accelerations are necessary in the unsteady case. The corresponding motions are fore and aft, yaw, heave or plunge and pitch.

$$c_{i\ \text{unsteady}} = f(\ddot{x},\ddot{y},\ddot{z},\frac{d\ddot{z}}{dx}\cdot x)$$

The similarity parameters for compressibility, viscosity and unsteadiness are:

$$c_{i\ \text{similarity}} = f(Ma_i, Re_i, k_i)$$

Trigonometric functions are not necessary to define angles of attack or yaw. The flow components due to different origin can be coupled directly by summation.

3. Critical Review Of Swept Wing Experiments

The extension of the existing twodimensional aerodynamic model starts with the consideration of the third flow component normal to the blade element plane. In the following only the lift or normal force coefficient is investigated.
If classical potential flow theory is applied there exists no influence. It is the well known independence principle. In real viscous flows a significant change of stall behaviour occurs but the linear aerodynamic regime seems to be unchanged. The reason of discussing the well established independence principle below stall are the fundamental experiments of St. Hilaire et al. (6),(7). These experiments with oscillating swept wings show an unknown effect as illustrated in Fig.2.

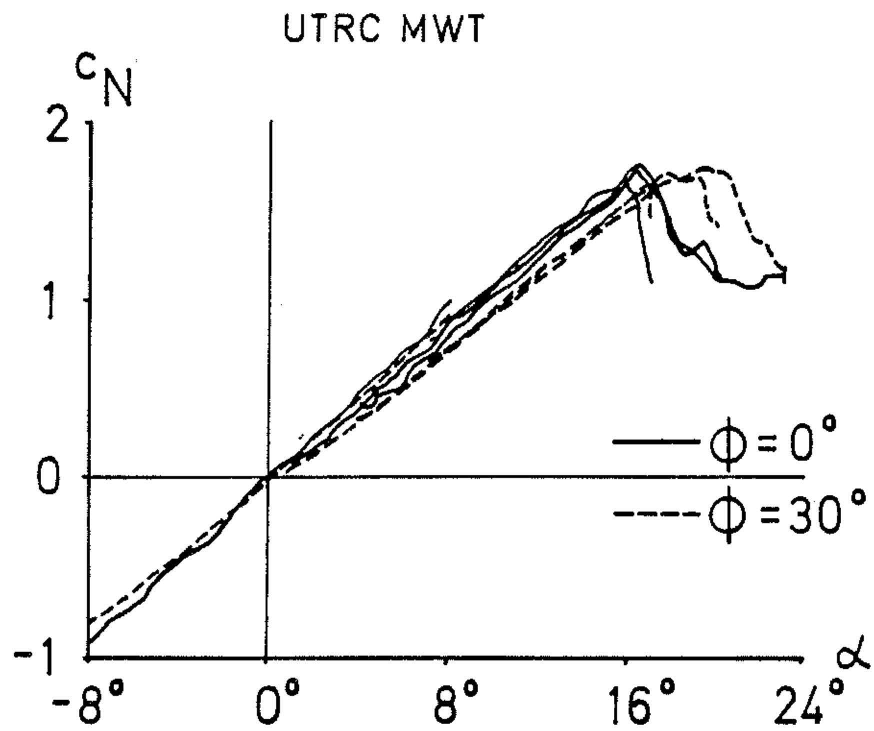

Fig.2 Curve slope drop effect at oscillating swept wing upstrokes

The upstrokes of the hystereses loops give lower c_l values in the swept wing case than in the unswept one.
A critical look at the full hystereses loops as presented in Fig.3 indicates two other differences. Swept wing hystereses are smaller than unswept and reach higher lift coefficients during the cycle. These differences are due to the steady influence of sweep. Stall onset occurs at higher angles of attack and therefore the hysteresis is smaller and the nonstalled lift range is extended.

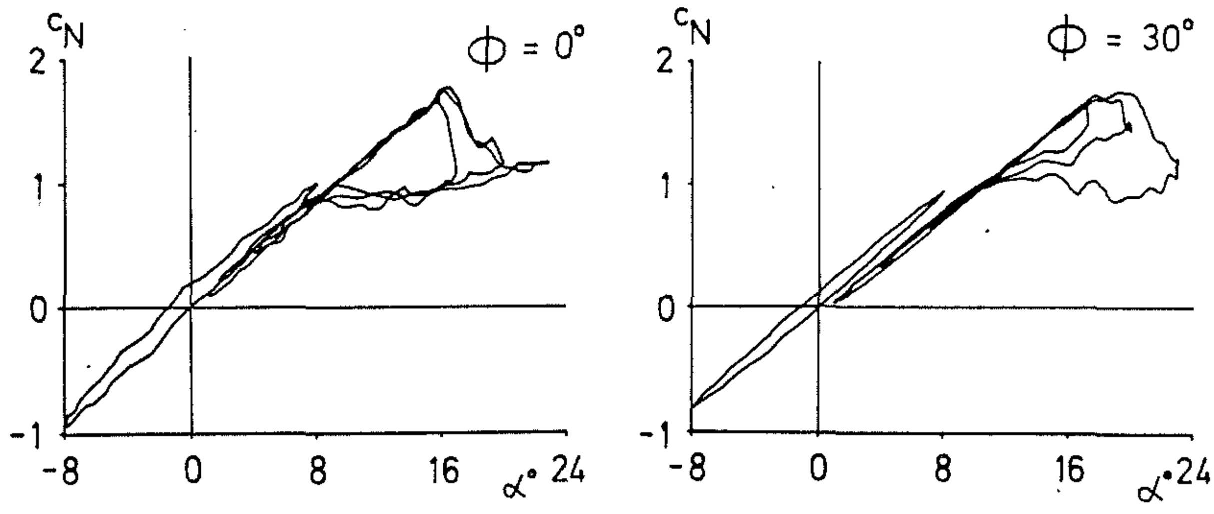

NACA 0012 UTRC MWT $M_c = 0.3$ $\bar{\alpha} = 8°$ $k = 0.05$

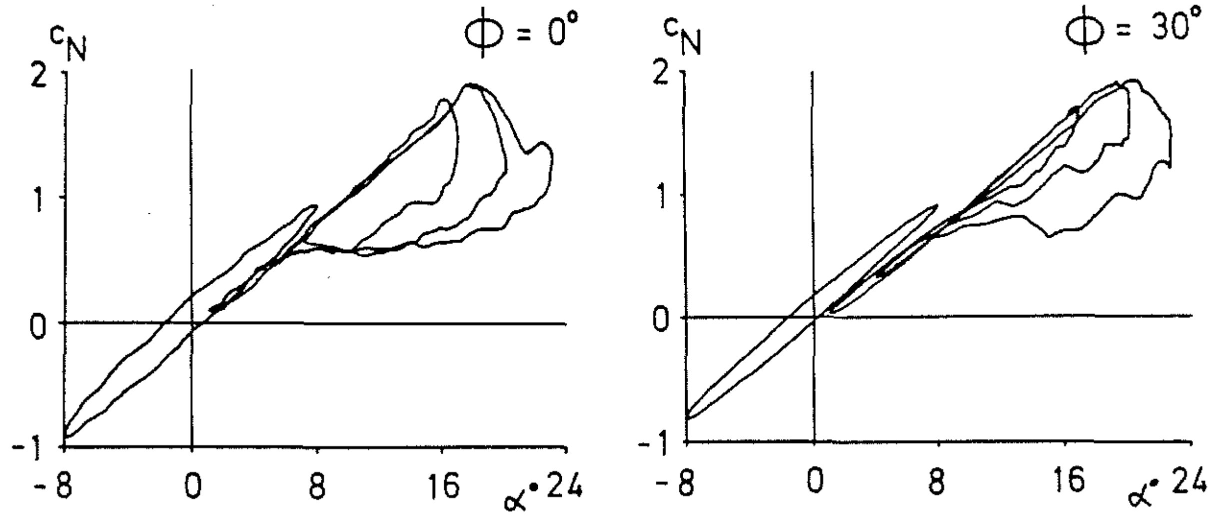

NACA 0012 UTRC MWT $M_c = 0.3$ $\bar{\alpha} = 8°$ $k = 0.1$

Fig.3 Swept and unswept oscillating wings (7)

However a drift of the measurement can be seen more detailed in Fig.4. The profile NACA 0012 is symmetric and consequently the hysteresis has to be symmetric for a mean angle of zero degrees. The magnitude of this drift should be considered carefully when analyzing new effects.
The next logical step is to look in detail at the steady difference between swept and unswept wings in the range of the classical independence principle. Fig.5 gives a light trend that steady swept wing lift curve slopes are below the unswept ones. The UTRC experiments were performed in the midspan of the wing. Is that the best location for the swept wing case? The old measurement of Dannenberg (8) contains different spanwise locations where pressure transducers were mounted. Indeed a strong lift variation exists in spanwise direction.

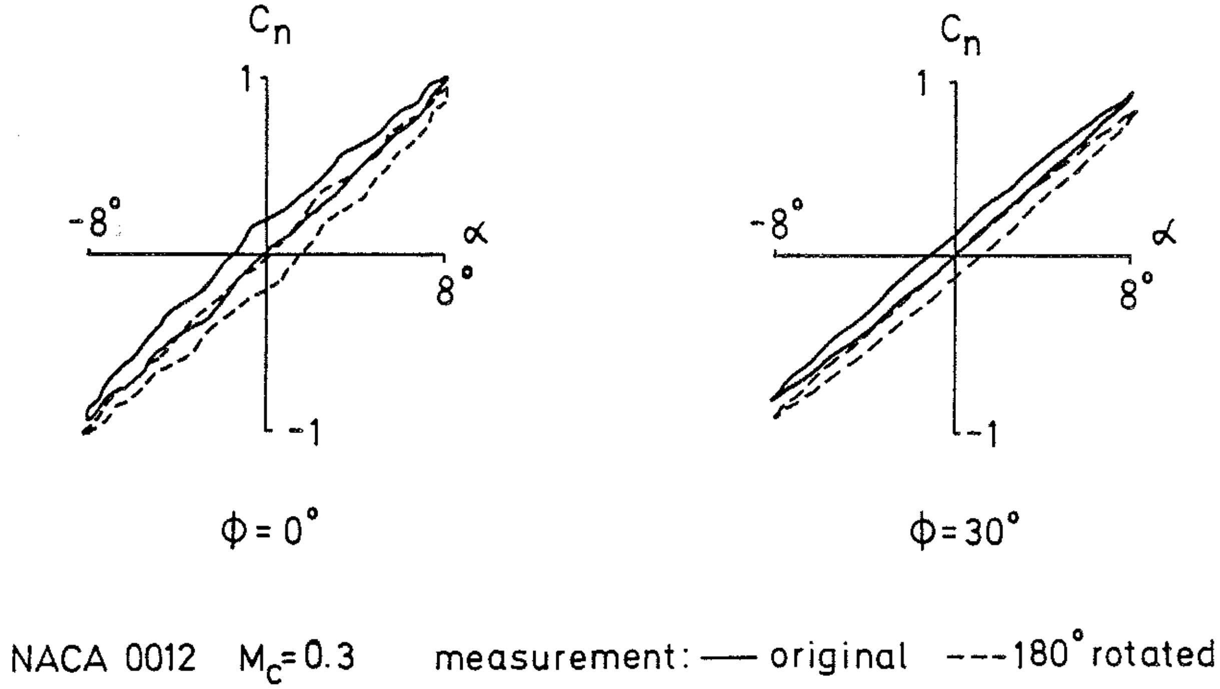

Fig.4 Measurement drift UTRC MWT (7)

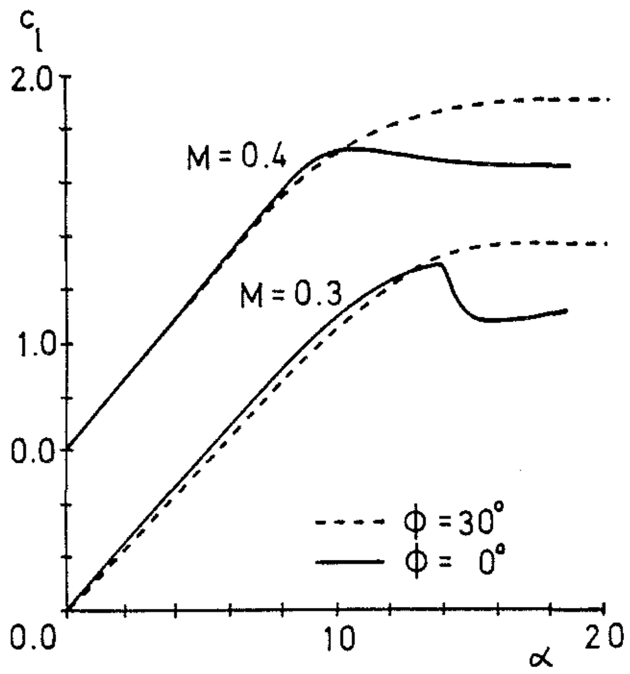

Fig.5 Steady difference between swept and unswept wings (7)

Following Fig.6 the inner 50 percent of the windtunnel were wall interference free. The corresponding lift curve slopes vary in the same magnitude as illustrated in Fig.2. To prove this result the wings of both investigations are compared in Fig.7. It should be noted that all corrections were removed for consistency with the uncorrected unsteady data of St.Hilaire et al. (6),(7)

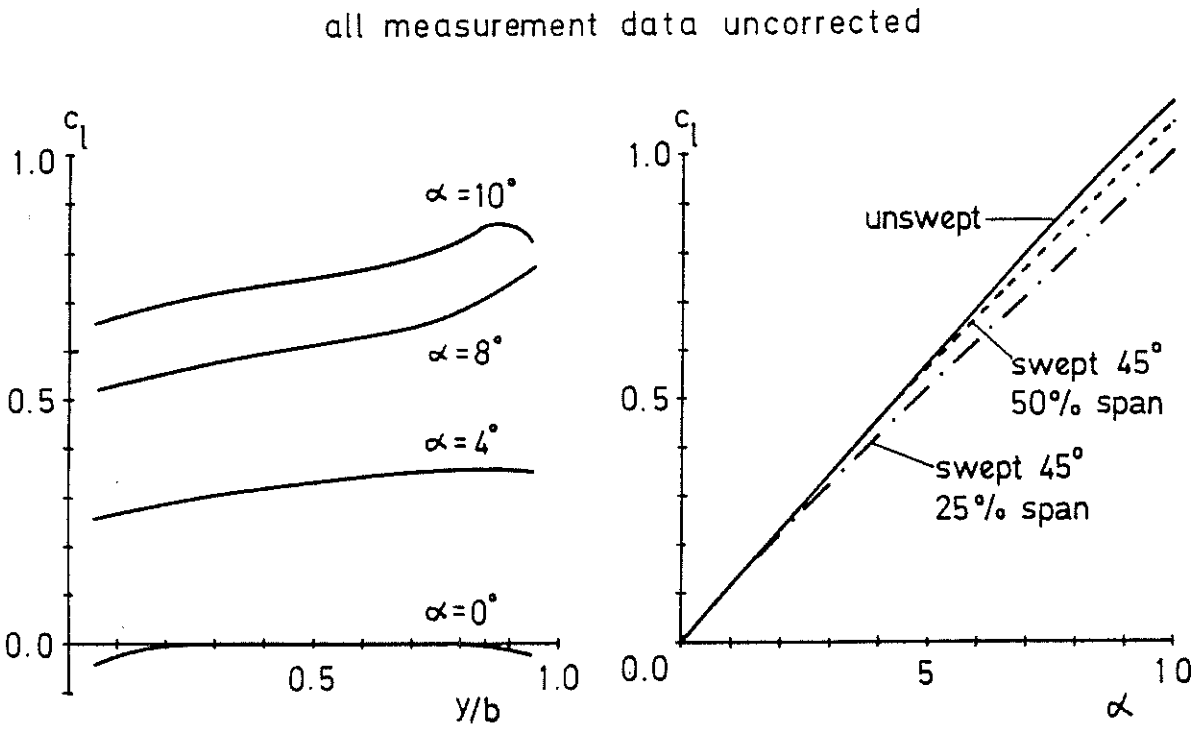

Fig.6 Spanwise trend of swept wing lift (8)

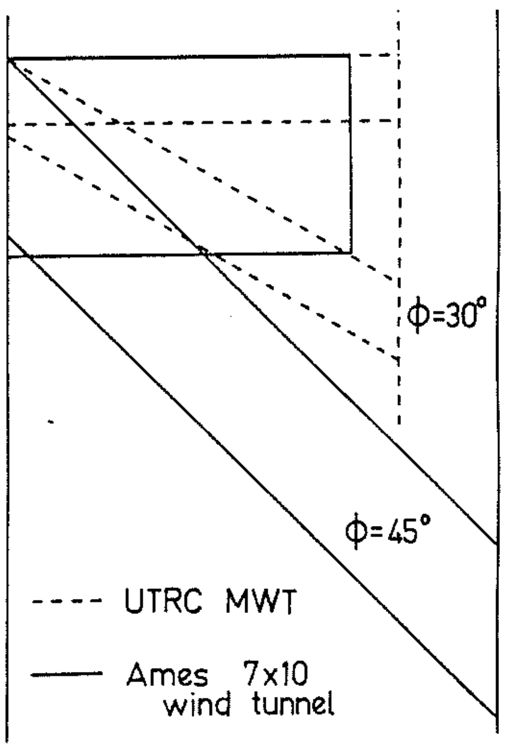

Fig.7 Comparison of windtunnels

The spanwise variation is assumed to be proportional to:

$$\Lambda / \cos^2\phi$$

In the present case the ratio Ames versus UTRC wind tunnel is one and hence the two experiments are supposed to be comparable in spanwise lift variation.

If the steady lift curve slope of the swept wing UTRC measurement (7) is corrected on this basis the upstrokes of the hystereses coincide with the steady curve. The independence of the upstroke slope on reduced frequency supports the interpretation that this new effect is just a steady one. It is recommended to perform steady swept wing experiments about 25 percent span where spanwise flow is small and no major wall effects occur. A low frequency unsteady swept wing experiment is the other possibility to obtain the equivalent steady behaviour. The statement of Wilby (9) that dynamic tests are needed to evaluate true steady stall incidence is then valid as well in the present case.

4. Steady Sweep Model

Till now the investigators of the oscillating swept wing experiments St. Hilaire and Carta (10),(11) did not present a model which accounts for the new swept wing effect. Therefore the existing twodimensional model (4) was extended. Two viscous effects exist. The well known stall delay is shown in Fig.8.

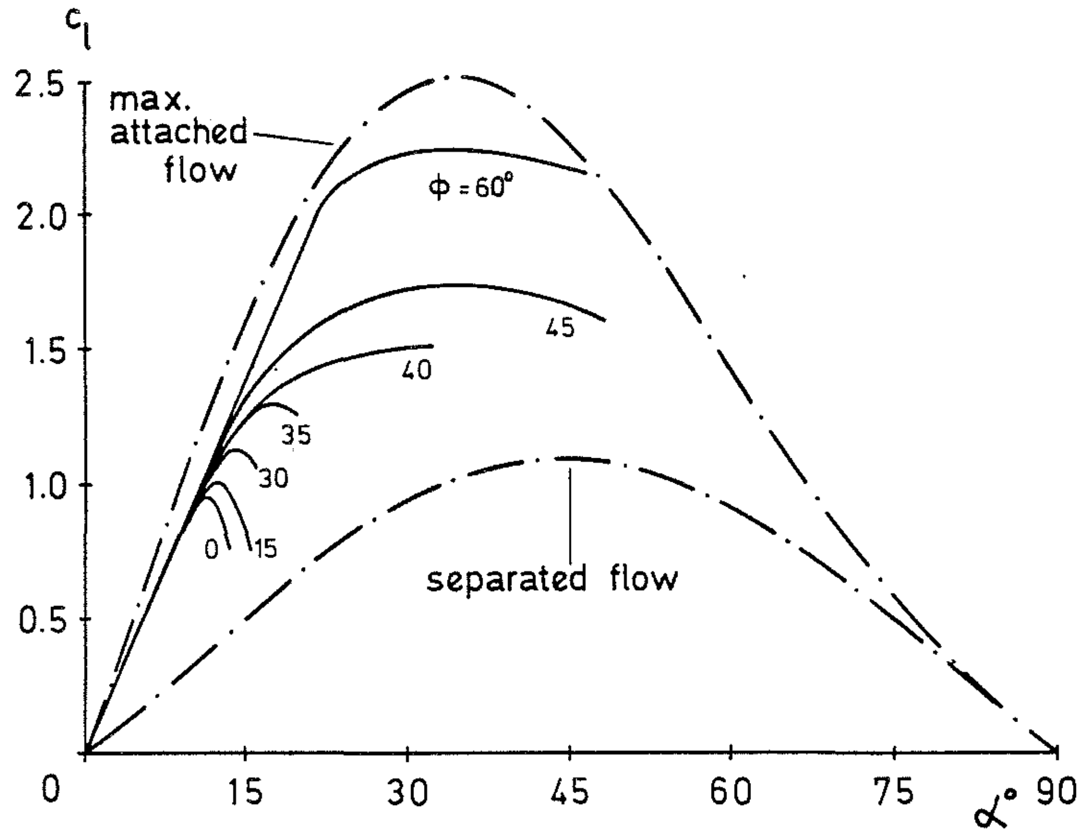

Fig.8 Stall delay of swept wings from (12)

The experiments were done by Purser and Spearman (12) on a yawed rectangular wing of aspect ratio 6. The data were reduced for comparison with the separated and attached flow limits.(5) The effect is modelled through movement of the maximum circulation point.

$$\Delta M_{zss} = c_{1y} \cdot (\dot{y})^2$$

The new lift curve slope drop effect is not indicated by the experiment. The chosen aspect ratio just fulfills the independence principle and is not a proof of the generality. However the measurement (12) results in higher lift curve slopes for lower aspect ratios and vice versa. Hence the effect is considered empirically in the following form:

$$\Gamma_{+,-} = \frac{M_{zss}^3 \cdot c_{ss}}{(M_z \pm M_{zss})^2 M_{zss} \cdot c_{ss} + c_{2y} \cdot (\dot{y})^2}$$

So the lift curve slope decreases with increasing sweep angle or yawed velocity and the shape of the curve is more rounded. The coefficient c_{2y} is evaluated from unsteady experiments.(7) The further simulation of swept oscillating airfoils is based on the unswept case and causes no problems.

5. The Impact Of Unsteady Sweep

The radial flow effects on rotor blades were well reviewed by Harris (13). Dwyer(14) and Mc Croskey (15) gave more details about boundary layers on rotating blades. Yet application beyond the independence principle is poor. Gormont(16)combined the improved engineering formulation of Harris with a fundamental blade stall model. Gangwani (17) reconstructed the UTRC oscillating swept wing data without analyzing the mechanisms involved. The recently formulated unified aerodynamic model of Peters,(18) based on ONERA work, does not include any sweep.

No model exists which considers the unsteady sweep. Fig.9 illustrates the sweep angle variation during one cycle for different radial stations in forward flight.

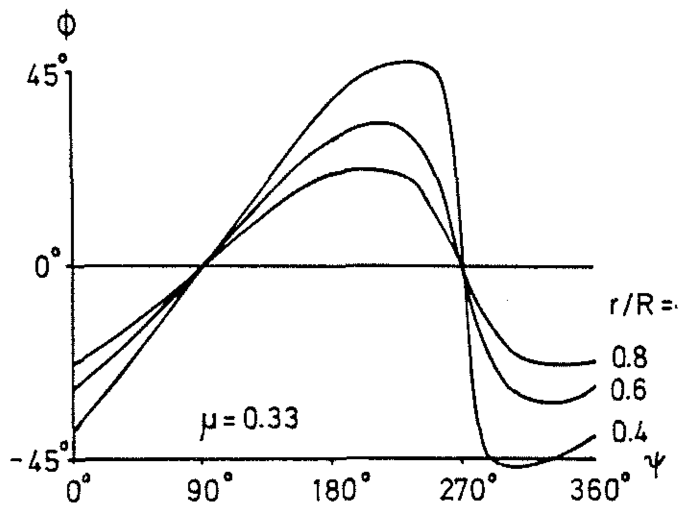

Fig.9 Sweep angle variation for different radial stations

The instantaneous radial flow component is only effective for a short period. Consequently the influence on the boundary layer is not fully developed. Fig.10 shows the impact of unsteady sweep compared with the quasisteady sweep assumption of Harris.(13) The remaining stall area on heavily loaded rotors moves to higher azimuth angles. The unsteady sweep influence interacting with the blade stall must be simulated to improve the understanding of the entirely unsteady rotor.

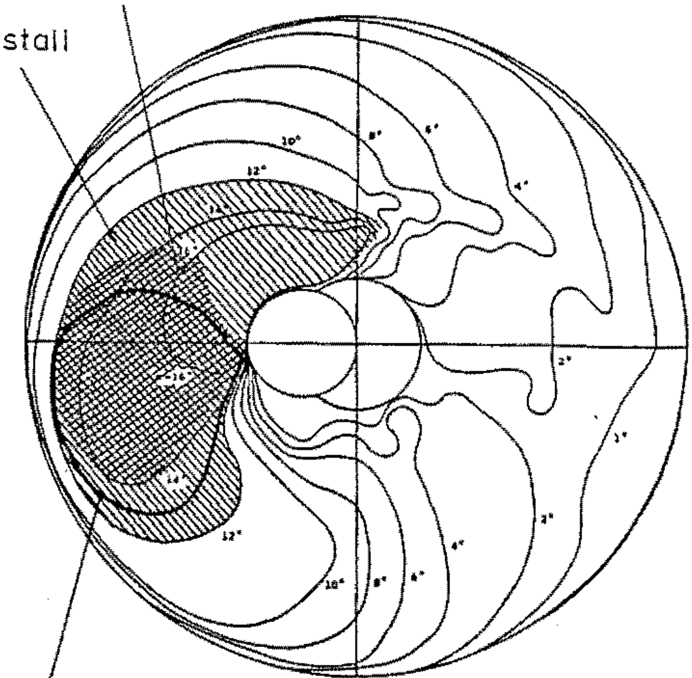

Fig.10 Influence of unsteady sweep on stall behaviour

6. Unsteady Sweep Model

The need of a simple preliminary unsteady sweep simulation model is due to the nonexistence of experiments. The steady sweep model of the present investigation utilizes the yaw velocity $\dot{y}$ instead of sweep angle ϕ. Hence the variation of $\dot{y}$ is almost harmonic. Fig.11 shows the typical delay behaviour. If $\ddot{y}$ or $\dot{\phi}$ is positive, the unsteady sweep curve lays below the steady one and vice versa. This law is presented in the form of the other viscous unsteady effects as described in Ref.(4).

$$\Delta\dot{y} = -c_y \cdot M_x \cdot c \frac{2a \cdot M_x \cdot \ddot{y}(t) \cdot c_{y45} + c \cdot \omega \cdot \ddot{y}(t - \frac{\pi}{2\omega})}{(c \cdot \omega)^2 + (2a \cdot M_x)^2 \cdot c_{y45}^2}$$

The empirical parameters c_y and c_{y45} need to be identified through future experiments.

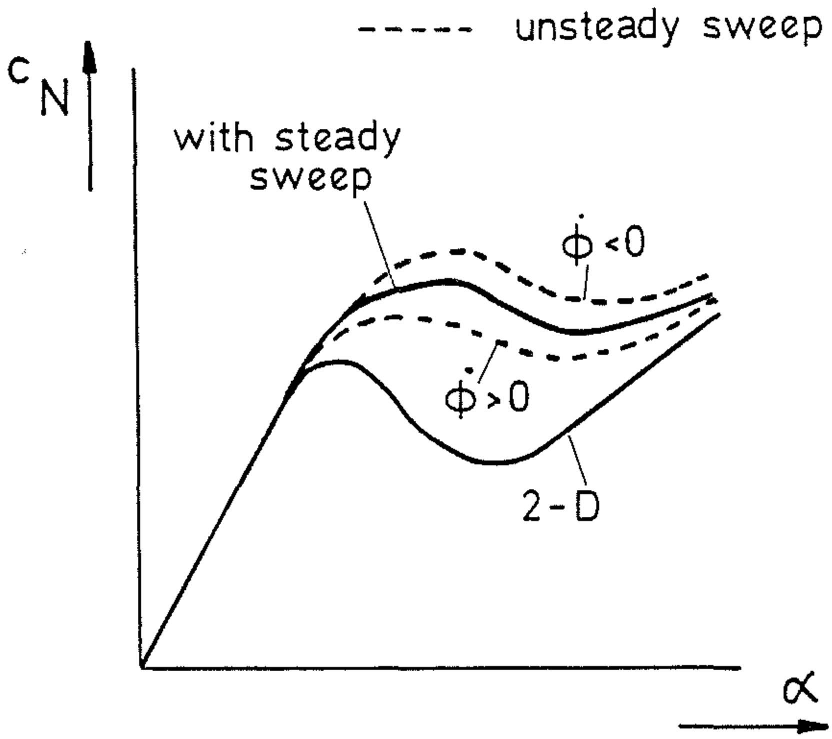

Fig.11 Unsteady sweep delay model

7. 3-D Effects Of The Finite Rotor Blade

Up to this point all steady and unsteady effects were considered at an element of the infinite rotor blade. At the real rotor blade tip and root the circulation decreases to zero. The common approach to these tip losses (19) is just a reduced blade length even within a highly advanced rotor analysis.(1) Only Harris et al. (20) prefer a linear lift decrease from a certain distance of the tip to zero at the tip.
The nonuniform spanwise circulation distribution and the strong tip gradient leads to a highly nonlinear trailing vortex sheet. The objective of the present investigation is to represent the tip loss and the solution of the complex integral equation associated with the vortex induced velocity, by a simple function.
Fig.12 shows the results of different methods for a constant and triangular twodimensional circulation distribution on a rectangular wing. The lifting line results of (21) are compared with more advanced theories from Wagner(22) and Urban(23) to consider the deviation trend in the new simple function.
The generalization of the geometry and load dependent 3-D influence is shown in Fig.13. The ratio of 3-D versus 2-D lift coefficient is used to model simultaneous the spanwise load and aspect ratio effects. The triangular circulation distribution, typical for helicopter rotors, results in almost the same reduction factor than for the constant circulation case.
The difference at midspan arises through the double triangular load of Ref.(21) and is not existent at a single rotor blade.

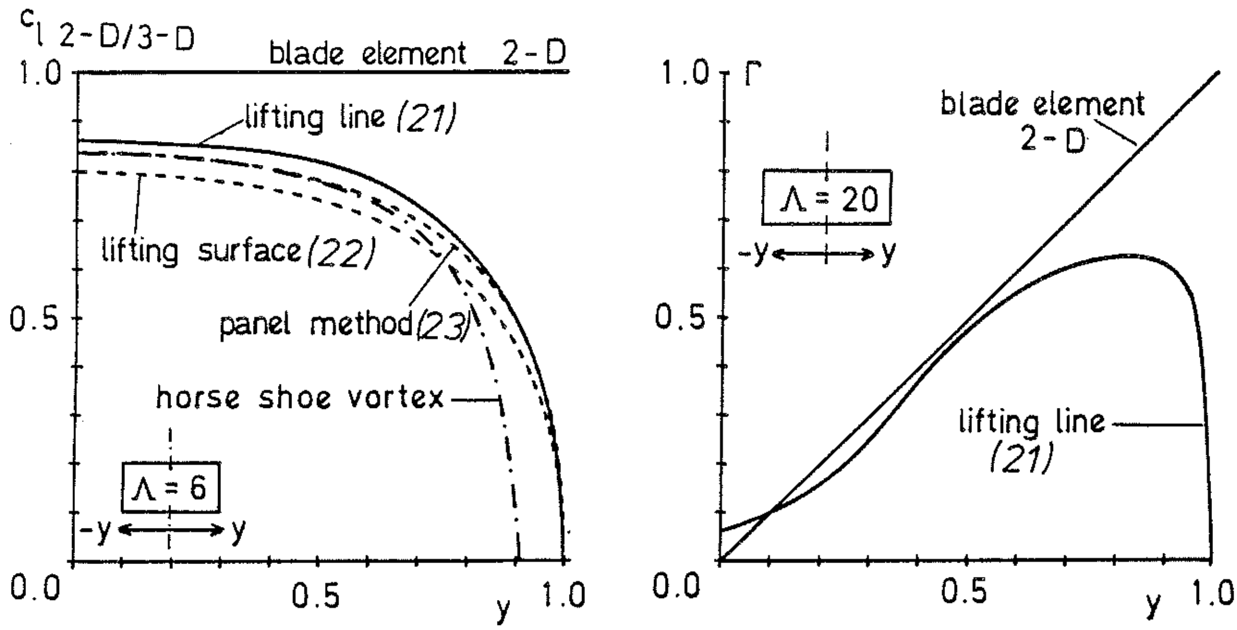

Fig.12 3-D influence on spanwise loading

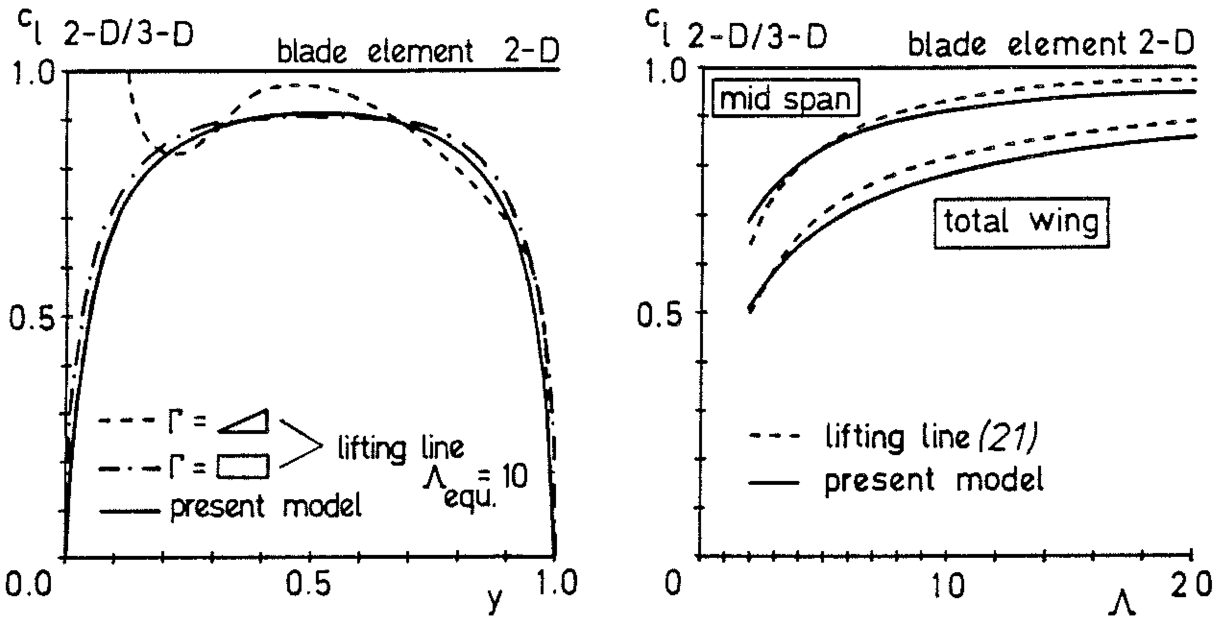

Fig.13 Comparison of the present model with theory

The following function leads to the appropriate simulation results of Fig.13.

$$c_{l\ 3\text{-}D} = c_{l\ 2\text{-}D}\ (y - y^2)/(1 - c_3 + c_3^2\cdot(y - y^2))$$

$$c_3 = 1 + 1/2\cdot\Lambda$$

This function is continuous and can be extended to unsteadiness for future. It should be noted that the rolled up trailing vortex sheet interacts with the blade at subsequent revolutions and is not included in the present model.

8. Analytical Integration Of Radial Loads

The total forces and moments of a rotor blade are normally obtained by numerical integration of the local blade element loads. The result depends on the appropriate choice of the number and location of blade elements especially when unsteady effects are involved. Further algorithms and logical decisions need computation time. Consequently analytical radial integration is introduced to avoid these disadvantages and to derive a general solution.
First of all velocity and acceleration components of the rigid blade depend on the y coordinate as follows:

$$\dot{x},\ddot{x} = f(y) \qquad \dot{y},\ddot{y} = \text{const} \qquad \dot{z},\ddot{z} = f(y,y^2)$$

The quadratic term of the normal component z is due to twist. Now the local blade loads can be written in terms of y. Fig.14 shows the typical integral over the dimensionless blade length.

$$F_i = \int_{y=0}^{1} \left[\begin{array}{l|l|l|l} \text{separated} & \text{separated} & \text{attached} & \text{vortex} \\ \text{displacement} & \text{circulatory} & \text{circulatory} & \text{effects} \\ & & & \\ \text{apparent} & \text{circulation} & \text{circulation} & \text{vortex} \\ \text{mass} \quad + & \text{lag} \quad + & \text{lag} \quad + & \text{proximity} \\ & & & \\ & & \text{unsteady} & \\ & & \text{viscous} & \end{array} \right] dy$$

Fig.14 Integration of steady and unsteady blade loads

The upper lines are the superimposed steady effects, the lower lines represent the equivalent unsteady flow phenomenas. The different terms can be integrated separately. This paper includes only explicit integration of the representative attached circulatory flow formula. The other terms are similar or trivial and therefore not presented.
The positive or negative circulation function (see Ref.4) is of the following degree:

$$\Gamma_{+,-} = \frac{(f(x,x^2))^3}{(z - f(x,x^2))^2 + f(x,x^2)^2}$$

The key fraction in terms of the integration variable is then

$$\int \frac{f(y^n)}{y^4 + b\cdot y^3 + c\cdot y^2 + d\cdot y + e}\, dy$$

The denominator equation of fourth degree consists of two conjugate complex roots

$$\int \frac{f(y^n)}{(y^2 + y\cdot s + t)\cdot(y^2 + y\cdot u + v)}\, dy$$

where:

$$g = \frac{\sqrt{|3bd - 12e - c^2|}}{3}\cdot\cos\left[\frac{\arccos\left(\dfrac{486\cdot(eb^2+d^2)-18c\cdot(9bd+72e-2c^2)}{(3bd-12e-c^2)^2\cdot\sqrt{|3bd-12e-c^2|}}\right)}{3}\right]$$

$$h = \sqrt{8g + b^2 - 4c} \qquad s = (b + h)/2 \qquad t = g + (bg - d)/h$$

$$u = (b - h)/2 \qquad v = g - (bg - d)/h$$

Now the fraction of fourth degree can be transformed in two fractions of second degree which are easy to integrate. On this basis the whole simulation model consists of fractions with denominators of second degree or lower. The contribution of unsteady viscous effects is limited to the same functional degree as shown above.

9. Application For Future Real Time Simulation

The significant progress of computers is one factor for use of more extensive real time simulation mathematical models. Nevertheless the other advance should come from the mathematical model itself. The present model is designed to be a contribution to this special topic.
Fig.15 shows the simple structure of parallel evaluation of mass and aerodynamic forces and moments. The input velocities and accelerations of the aerodynamic module can be used directly without transformation in an aerodynamic coordinate system. The present formulation is highly appropriate for parallel processing. The same basic structure is used for all rotor blades, tail plane or wing. The continuous representation of the aerodynamic behaviour should help to avoid divergency in the simulation process. Saving logical decisions the synchronization of the numerous processors can be done more effective.

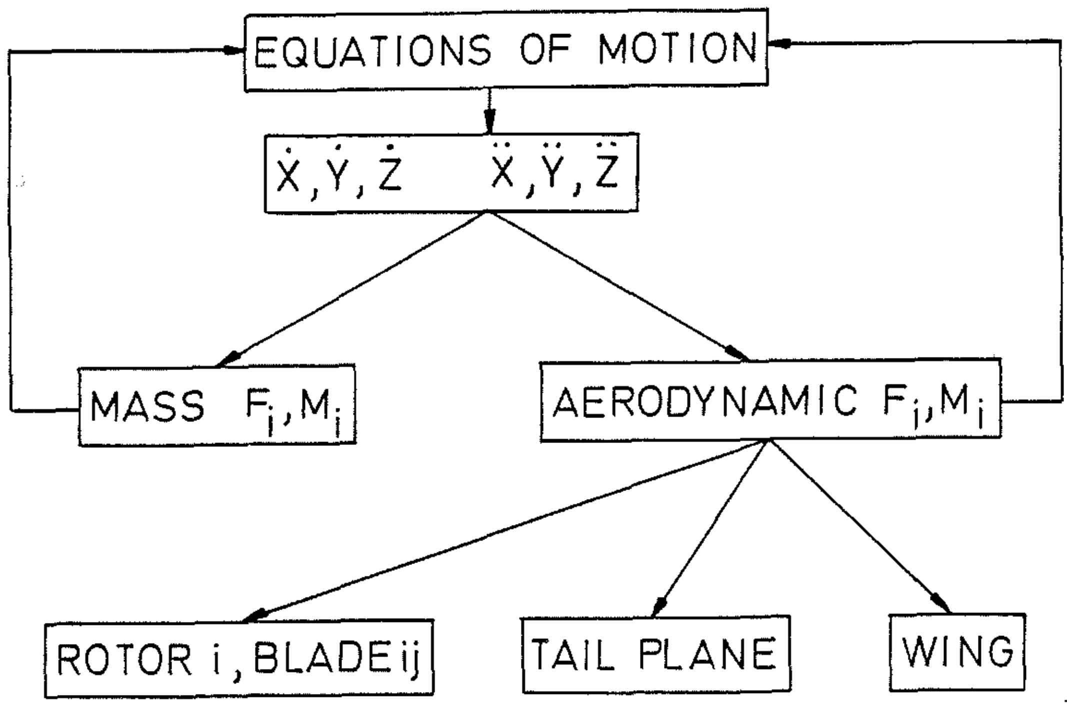

Fig.15 Application of the general aerodynamic module

10. Conclusions

A general formulation has been developed to describe the aerodynamic forces and moments of a threedimensional rotor blade in steady and unsteady, separated and attached flow. The major findings are:

1) The modular structure of a 2-D model allows consistent extension to 3-D.
2) Simple theories and empirical parameters with physical content replace complex numerical methods.
3) Simulation of heavy loaded rotors requires a simple model of all unsteady viscous effects.
4) Analytical expressions allow subsequent optimization studies.
5) Fixed blade elements are no longer necessary.
6) Application for real time simulation indicates substantial improvement.
7) Unsteady sweep experiments are necessary to verify and improve the preliminary model.
8) Vortex interaction problem should be included for future.

Acknowledgement

The paper is based on research work funded by the Bundesministerium für Forschung und Technologie BMFT (Ministry of Research and Technology), contract LFF 83408.

References

1) Johnson, W., Development of a comprehensive analysis for rotorcraft -I,Rotor model and wake analysis, Vertica, Vol.5, pp 99-129, 1981

2) Williams, L., Real time blade element rotor modelling, Proc. of the international conference on Flight Simulation of Helicopters Status and Prospects, Royal Aeronautical Society, London, 1985

3) Offenbeck, H.G., Dahl, H.J., Helicopter simulation for design, Proc. of the international conference on Flight Simulation of Helicopters Status and Prospects, Royal Aeronautical Society, London, 1985

4) Leiss, U., A consistent mathematical model to simulate steady and unsteady rotor-blade aerodynamics, Proc. of the 10th European Rotorcraft Forum, Paper No.7, The Haag, The Netherlands, 1984

5) Leiss, U., Semi-empirical simulation of steady and unsteady rotor blade aerodynamic loading, Proc. of the international conference on rotorcraft basic research, Raleigh, Research Triangle Park, 1985

6) St. Hilaire, A.O., Carta, F.O., Fink, M.R., Jepson, W.D., The influence of wing sweep on the aerodynamic loading of an oscillating NACA 0012 airfoil, Vol I - Technical Report, NASA CR-3092, 1979

7) St. Hilaire, A.O., Carta, F.O., The influence of sweep on the aerodynamic loading of an oscillating NACA 0012 airfoil, Vol II - Data Report, NASA CR-145350, 1979

8) Dannenberg, R.E., Measurements of section characteristics of a 45° swept wing spanning a rectangular low speed wind tunnel as affected by the tunnel walls, NACA TN 2160, 1950

9) Wilby, P.G., The aerodynamic characteristics of some new RAE blade sections and their potential influence on rotor performance, Vertica, Vol.4, pp 121-133, 1980

10) St. Hilaire, A.O., Carta, F.O., Analysis of unswept and swept wing chordwise pressure data from an oscillating NACA 0012 airfoil experiment, Vol I - Technical Report, NASA CR-3567, 1983

11) Carta, F.O., Dynamic stall of swept and unswept oscillating wings, AGARD CPP 386, paper 2, Göttingen, 1985

12) Purser, P.E., Spearman, M.L., Wind tunnel tests at low speed of swept and yawed wings having various planforms, NACA TN 2445, 1951

13) Harris, F.D., Preliminary study of radial flow effects on rotor blades, Journal of the American Helicopter Society, Vol.11, No.3, July 1966

14) Dwyer, H.A., Mc Croskey, W.J., Crossflow and unsteady boundary -layer effects on rotating blades, AIAA Journal, Vol.9, No.8, August 1971

15) Mc Croskey, W.J., Measurements of boundary layer transition, separation and streamline direction on rotating blades, NASA TN D-6321, April 1971

16) Gormont, R.E., A mathematical model of unsteady aerodynamics and radial flow for application to helicopter rotors, USAAMRDL Technical Report 72-67, 1972

17) Gangwani, S.T., Prediction of dynamic stall and unsteady airloads for rotor blades, Journal of the American Helicopter Society, October 1982

18) Peters, D.A., Toward a unified aerodynamic model for use in rotor blade stability analyses, Proc. of the 40th Anual Forum of the American Helicopter Society, Washington D.C.,1984

19) Gessow, A., Myers, G.C., Aerodynamics of the Helicopter, Frederic Ungar Publishing Co., New York, 1967

20) Harris, F.D., Kocurek,J.D., McLarty, T.T., Trept,Jr.,T.J., Helicopter performance methodology at Bell Helicopter Textron, Proc. of the 35th Annual Forum of the American Helicopter Society, Washington D.C., 1979

21) Abbott, I.H., von Doenhoff, A.E., Theory of wing sections, Dover Publications Inc., New York, 1958

22) Wagner, S., On the singularity method of subsonic lifting-surface theory, Journal of Aircraft, Vol.6, No.6, 1969

23) Urban, Ch., Berechnung der nichtlinearen aerodynamischen Kräfte und Momente interferierender Tragflächen, Universität der Bundeswehr, Institut für Luftfahrttechnik IB 83-1, Neubiberg, 1984

24) Bronstein, I.N., Semendjajew, K.A., Taschenbuch der Mathematik, Verlag Harri Deutsch, Zürich und Frankfurt/Main, 1975